PHYSICAL REVIEW B VOLUME 26, NUMBER 6 15 SEPTEMBER 1982

Thermal transport properties of $SbCl_5$ graphite

M. Elzinga, D. T. Morelli, and C. Uher*
Department of Physics, University of Michigan, Ann Arbor, Michigan 48109
(Received 29 April 1982)

Thermopower and thermal conductivity have been measured between 2 and 300 K on $SbCl_5$ graphite intercalation compounds spanning the stages 2—10. In addition, a strong transverse magnetic field has been used to separate the electronic and lattice parts of the thermal conductivity. The thermopower of all compounds is positive and increases with stage index. An anomaly near 230 K is associated with the commensurate-incommensurate transition. The thermal conductivity at high temperatures increases with the stage index but is significantly smaller than the conductivity of pure graphite. However, below about 5 K, the thermal conductivity of the intercalated material is larger than that of graphite due to as much as an order-of-magnitude enhancement in their electronic thermal conductivity. The lattice thermal conductivity of the intercalation compounds is smaller than that of graphite but it shows a surprising stage and temperature dependence which suggests that the low-frequency lattice modes of intercalant provide a significant contribution, particularly at low temperatures.

I. INTRODUCTION

The study of graphite intercalation compounds (GIC's) is currently an intensively pursued area of solid-state physics and material science. In a relatively short time, a large amount of information has been gathered on the structural and electronic properties of these materials[1] and headway has been made in understanding their unusually high electrical conduction.[2] On the other hand, investigations of thermal properties, notably thermal conductivity and the thermoelectric power, are sparse. Ubbelohde[3] measured the thermopower of HNO_3 graphite down to about 200 K and, most recently, the Louvain group in collaboration with the MIT group investigated the thermal properties of a few samples of $FeCl_3$ graphite[4] and a stage-5 potassium graphite.[5]

We have undertaken measurements of the thermal conductivity and thermopower on samples of highly oriented pyrolytic graphite (HOPG) intercalated with $SbCl_5$, spanning the stages 2 to 10 and a temperature range 2—300 K. $SbCl_5$ forms the most air-stable acceptor-type GIC and this is one of the reasons why we have chosen it for the thermal transport investigations. Furthermore, the structure and its stage and temperature dependence have been well established by studies at this institution[6] and elsewhere.[7,8] Most recently we have reported[9] on the occurence of a commensurate $(\sqrt{7}\times\sqrt{7})$ to incommensurate transition at around 230 K for stages $N \geq 2$ which was accompanied by an anomalous and strongly hysteretic resistivity contribution.

Thermal conductivity and thermopower measurements are powerful tools which can provide an insight into several fundamental phenomena (contribution of electrons and phonons, elasticity of scattering, phonon-drag effect, etc.) which govern the transport properties of solids and which are either difficult or outright impossible to obtain by any other means. In this paper we apply these techniques to a systematic investigation of $SbCl_5$ graphite intercalation compounds and report on our findings.

II. EXPERIMENTAL

Thermopower and thermal conductivity were determined by a steady-state technique over the temperature range 2—300 K. Samples were prepared by the standard two-temperature-zone method in vapor. Starting materials were Union Carbide HOPG graphite and high-purity $SbCl_5$. Sample dimensions were in the range $30\times2\times0.5$ mm^3. Typical intercalation temperatures for various stages are given in Table I. We have not succeeded in preparing a sufficiently large and homogeneous sample of stage-1 material, nor stages higher than 5 with one exception of a stage-10 sample. However, all samples investigated in this report are pure stages as confirmed by (00*l*) x-ray scans made on several different regions of each

TABLE I. Some parameters of interest for $SbCl_5$ graphites.

Stage	Growth conditions $T_{graphite}$ (°C)	Growth conditions T_{SbCl_5} (°C)	Coefficients of diffusion thermopower (10^{-8} V K^{-2})	Residual resistivity (10^{-9} Ω m)
2	200	200	3.0	
3	200	100	5.5	11.1
5	200	60	8.0	5.7
10	200	30	21.1	6.4

sample. An example of such a scan on a stage-5 sample is given in Fig. 1. As we have already noted, $SbCl_5$ graphites are unusually air-stable compounds and show no deterioration even after prolonged exposure to air. Furthermore, the compounds can be held in high vacuum without any detectable change, an important feature for thermal conductivity measurements where adiabatic conditions are required.

Unlike electrical resistivity, which can be measured without making any contact to the sample, investigation of the thermal transport properties necessitates the attachment of a sample heater, thermometers and thermopower voltage probes. Since $SbCl_5$ is a highly reactive acid, great care must be exercised in the choice of contacts. Copper, for instance, appears to be strongly attacked by this intercalant. We have found that platinum is very stable in $SbCl_5$ acid and have therefore used it to make contacts to intercalated samples by forming small, light clamps. The heater (small metal film resistor) and thermometers are easily soldered to these clamps with a very low melting point solder (40 °C). Thermopower voltage probes were high-purity Pb wires which were

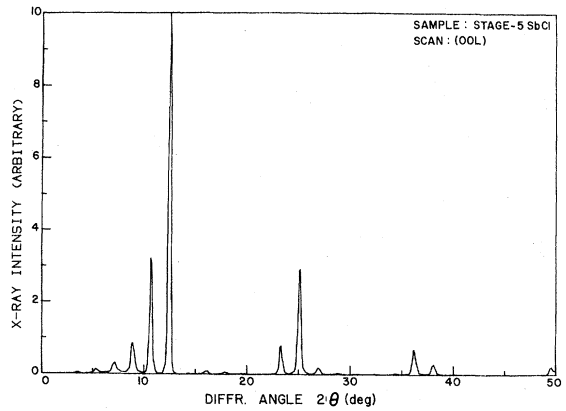

FIG. 1. Typical (00l) x-ray scan for a stage-5 $SbCl_5$ graphite.

squeezed between the sample and Pt clamps. In order to keep the heat loss minimal, these Pb probes were always removed when the thermal conductivity was measured. We have observed no corrosion effects of $SbCl_5$ on Pb probes. Lead has an additional advantage of being a reference thermopower material. Tables of Roberts[10] were used to correct for its emf contribution in zero magnetic field and the effect of magnetic field was subtracted using the data of Caplin *et al.*[11] Thermopower voltages are measured by a Keithley nanovoltmeter with a sensitivity of about 3×10^{-9} V.

A choice of thermometers is important in any thermal conductivity measurements. It becomes absolutely critical when the effect of magnetic field on the thermal transport is studied. Carbon-glass thermometers, by virtue of their very small and reproducible magnetoresistance, are essentially the only suitable sensors. In selecting a pair of such thermometers one requires that the resistance of "hot" and "cold" sensors satisfy as closely as possible the condition

$$R_H(T,B)\approx R_C(T,B)\ , \tag{1a}$$

i.e., they have not only near the same resistance but, more important, the effect of the field is identical on both sensors. Our pair of sensors was selected from a batch of about a dozen according to the above criterion and the zero-field calibration was made against a reference Ge thermometer calibrated in the National Measurement Laboratory in Sydney. Magnetoresistance of both sensors is identical to within 0.1% and, in the field of 6.5 tesla, represents a shift of 18 mK at 4.2 K. These shifts are only weakly temperature dependent and they can be corrected by running several calibration sweeps at different fixed temperatures.

In materials which have substantial electronic thermal conductivity the application of transverse magnetic field will result in higher thermal resistance of the sample over its zero-field value and, consequently, in a large shift of its mean tempera-

ture if the heater power stays constant. To prevent this and thus to ensure that the separation of the thermal conductivity is carried out at a constant temperature, the temperature difference $\Delta T = T_H - T_C$ (voltages V_H and V_C measured on digital voltmeters for a constant thermometer current) must be kept fixed as the field increases. This is achieved by gradually reducing the sample heater power and making a small adjustment on an auxiliary heater at every preset field value. The magnetic field is generated by a 6.5-T split-coil superconducting solenoid which has a 3-cm radial port. This solenoid is supported on a turntable and the field can be rotated to any desired position with accuracy better than 0.5°. We take the maximum of the angular dependence of the resistivity as a reference for the orientation of the field $\vec{B}$ parallel to the c axis of each sample.

A gold-plated oxygen-free high conductivity (OFHC) copper cylinder is placed around the sample and is screwed to the cold tip of the cryostat. It serves as a radiation shield for thermal conductivity measurements at higher temperatures. Overall, we estimate the error on our thermal conductivity data of about 0.5% below 77 K and about 2% near room temperature.

III. RESULTS AND DISCUSSION

A. Thermopower

The overall temperature dependence of the in-plane thermopower of $SbCl_5$ graphites is illustrated in Fig. 2. For comparison, we also include the data on the in-plane thermopower of the parent material, HOPG, and its exfoliated version known as *ZYX* graphite.[12] Several features are immediately apparent:

(i) The thermopower of all $SbCl_5$ graphites is positive throughout the entire temperature range investigated. This is in accord with the underlying mechanism of the charge transfer upon intercalation with $SbCl_5$ which is believed to proceed via a disproportionate reaction similar to that of AsF_5 compounds,[13] namely

$$3SbCl_5 \rightarrow 2SbCl_6^- + SbCl_3 + 2e^+ \,. \qquad (1b)$$

In fact, the lack of any sign of a negative anomaly at low temperatures which is typical for HOPG and which is also clearly evident in a weakly p-type (residuum with $p/n = 1.2$) *ZYX* graphite suggests that $SbCl_5$ compounds (even for stages as high as 10) are strongly uncompensated p-type systems. This contradicts the interpretation of the

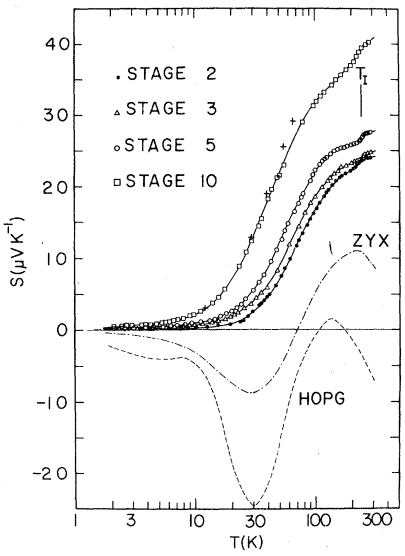

FIG. 2. Temperature dependence of the in-plane thermopower of $SbCl_5$ graphites. Dashed curve indicates the in-plane thermopower of HOPG and chain curve is the thermopower of (exfoliated) *ZYX* graphite. Crosses designate the magnetothermopower of a stage-10 compound at 6 tesla. T_I marks the temperature of the commensurate-incommensurate transition.

magnetothermal oscillations observed by Batallan *et al.*[14] on stages 2 and 4 which concludes that these acceptor compounds are compensated.

(ii) The thermopower increases with increasing stage. This, we believe, is due to a gradual decrease of the carrier degeneracy and an increase in mobility as the stage increases. Such a trend is particularly noticable for a stage-10 compound. Again, this feature is not in accord with the interpretation of Batallan *et al.* which claims stage independence of the Fermi surface. On the other hand, the most recent de Haas–van Alphen (dHvA) data on stages 2, 3, and 4 of $SbCl_5$ graphite by Takahashi *et al.*[15] show clearly that the dHvA spectra *are* stage dependent and, consequently, a stage dependence of the transport properties is not unexpected.

(iii) Near 230 K we observe an anomalous hump on the thermopower curves of all intercalated samples. This occurs at about the same temperature where the commensurate $\sqrt{7}\times\sqrt{7}$–incommensurate transition occurs in the intercalated layers, as demonstrated recently by x-ray scattering and electrical resistivity measurements.[9] We thus associate the thermopower anomaly with this same physical phenomenon.

(iv) At liquid-helium temperatures the thermopower reaches submicrovolt K^{-1} values which are

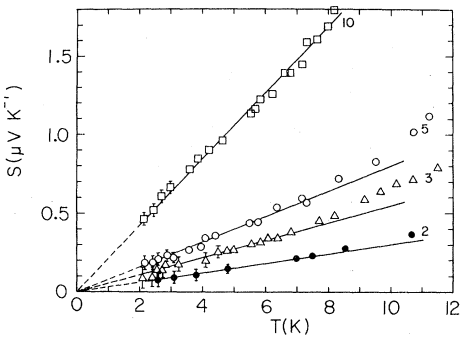

FIG. 3. Detailed behavior of the thermopower at low temperatures. Slopes of the straight lines are given in Table I.

typical of good metals and below about 7 K the data fall on straight lines which extrapolate to $S=0$ as T approaches absolute zero (Fig. 3). The thermopower for a multicarrier system is given by

$$S=\frac{\sum_i \sigma_i S_i}{\sum_i \sigma_i} , \tag{2}$$

where σ_i and S_i are the electrical conductivity and the partial thermopower of the ith type of carriers. For a strongly degenerate system the diffusion thermopower associated with the ith carrier pocket is

$$S^i_{\text{diff}}=\pm\frac{\pi^2 k_B^2}{3e}\frac{T}{E_F^i} , \tag{3}$$

where k_B is the Boltzmann constant and E_F^i is the Fermi energy. From the observed linear variation of the thermopower at the lowest temperatures we conclude that the thermopower is governed by the carrier diffusion mechanism and the coefficients of the linear terms are given in Table I. Unfortunately, due to a lack of detailed information on the shape and the multiplicity of the Fermi surface of these compounds, at the present time it is not possible to estimate the Fermi energy for each compound from the coefficients of the linear terms. This would only be admissable in the case that the compounds have a single carrier spectrum.

(v) Above 8 K, deviations from the linear variation of the thermopower with temperature are clearly visible. Such low-temperature deviations are usually explained by invoking the phonon-drag effect, i.e., the total thermopower is assumed to vary as

$$S=S_{\text{diff}}+S_{\text{drag}}=AT+BT^n , \tag{4}$$

where the exponent n reflects the behavior of the specific heat at low temperatures, typically $n=3$. The deviations in Fig. 3 could, indeed, be fitted reasonably well with $n=3$ up to about 20 K. However, for the graphite intercalation compounds, this is probably nothing more than a fortuitous fit. It is a well-established fact that the specific heat of graphite[16] as well as of $SbCl_5$ graphites[17] follows an approximately T^2 dependence rather than the more usual T^3 variation. One should thus exercise caution in interpreting the deviations as the sign of a phonon drag acting on the holes; it could, if two or more carriers are present, merely reflect the temperature variation of the mobility ratio.

(vi) We have attempted to measure the thermopower in a transverse magnetic field at several temperatures up to about 70 K. Contrary to the case of HOPG, the magnetic field has very little effect on the thermopower of $SbCl_5$ graphites. Above 10 K, the magnetothermopower of a stage-10 compound is small and positive and its value at 6 tesla is indicated in Fig. 2 by crosses. The magnetothermopower of lower-stage samples is even smaller. This rather uneventful behavior of the magnetothermopower indicates that the intercalated samples are strongly degenerate with small mobilities.

B. Thermal conductivity

In general, thermal conduction in a solid proceeds via two processes, lattice vibrations and free-carrier transport. The relative strength of these two heat transport mechanisms depends very strongly on whether one is dealing with metals or insulators. There is, however, a class of solids, namely semiconductors and semimetals, where the two processes are usually of equal importance, at least in some temperature range. The total thermal conductivity can then be written as

$$K=K_L+K_E , \tag{5}$$

where K_L and K_E are the lattice and electronic contributions, respectively.

In pure graphite the lattice thermal conductivity dominates over most of the temperature interval, the electronic contribution becoming significant only at and below liquid-helium temperature.[18] Upon intercalation, the carrier density of the intercalated material is enhanced by 2–3 orders of magnitude and the in-plane electrical conductivity reaches values as much as 10–15 times larger than those of pristine graphite.[19] Thus we also expect a

significant increase in the electronic part of the thermal conductivity of intercalated compounds over that of pure graphite. Since the electronic and lattice thermal conductivities differ strongly in their temperature dependence and the phonons are likely to be strongly scattered by defects introduced by intercalation, this should also lead to markedly different temperature dependence of the thermal conductivity of GIC's.

The data are presented in Fig. 4. For comparison, the thermal conductivity of HOPG is indicated by a dashed curve and that of *ZYX* graphite[20] by a chain curve. At high temperatures the thermal conductivity of all $SbCl_5$ graphites is substantially smaller than that of HOPG and decreases with increasing intercalant concentration. This we explain in terms of strong phonon-defect scattering, particularly for low-stage compounds, which more than offsets any electronic thermal conductivity enhancement associated with increased charge carrier density. We notice further that the peak in the thermal conductivity curves shows a distinct shift towards lower temperatures, closer to the peak of HOPG, as the stage increases. Thus, we conclude that at higher temperatures, certainly above 100 K, the phonons are the dominant heat transport mechanism in $SbCl_5$ intercalated graphites even though this is significantly reduced compared to HOPG. Below 100 K the temperature dependence of the thermal conductivity is different from that of HOPG. It follows an approximately linear variation with T, somewhat more rapid for dilute stages especially at higher T, and somewhat weaker for stage 2. This is to be compared to the $T^{2.5}$ law of HOPG. Consequently, in the liquid-helium temperature range, the thermal conductivities of all the measured $SbCl_5$ graphites become higher than the conductivity of HOPG. We also observe that the stage dependence of the conductivity in this range becomes substantially smaller than near room temperature and, in fact, the stage-10 sample shows lower conductivity than the stage-5 sample. The magnitude of the conductivities as well as the trend in their stage dependence suggests that the electronic thermal conductivity now becomes more important than the phonon's contribution. To elucidate this point further and to get a quantitative estimate of the importance of phonons and carriers we have used a strong transverse magnetic field to separate the thermal conductivity into its lattice and carrier contributions.

A premise of this technique is that the magnetic field will reduce the electronic part of the conductivity while having no effect on the phonons. A condition for suppression of the electronic part of the thermal conductivity is that

$$\omega\tau=\mu B \gg 1 , \tag{6}$$

i.e., that the field is sufficiently strong to achieve a classical high-field regime. ω, τ, μ, and B are, respectively, cyclotron frequency, relaxation time, mobility, and the magnetic field strength. The dependence of the thermal conductivity on magnetic field at 4.5 K is shown in Fig. 5 and in Fig. 6 are given magnetoconductivities of a stage-10 sam-

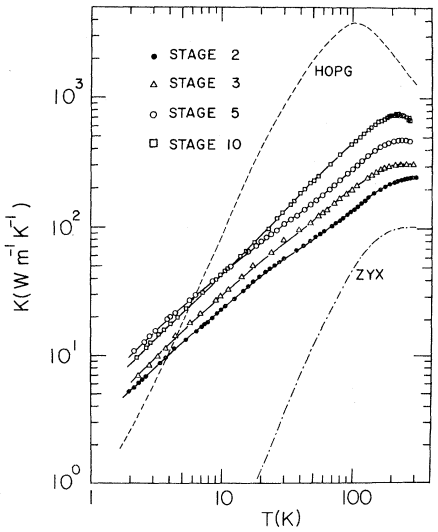

FIG. 4. Overall temperature dependence of the in-plane thermal conductivity. HOPG is designated by dashed curve and *ZYX* by chain curve.

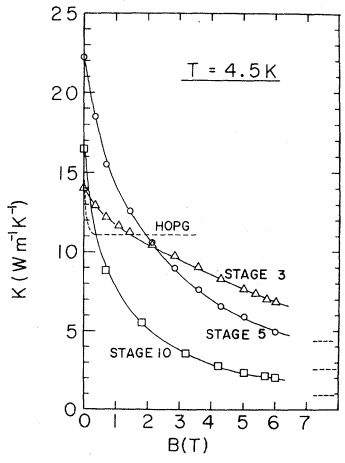

FIG. 5. Magnetothermal conductivity of $SbCl_5$ graphite and HOPG at 4.5 K. High-field asymptotes are indicated by broken lines on the right-hand side.

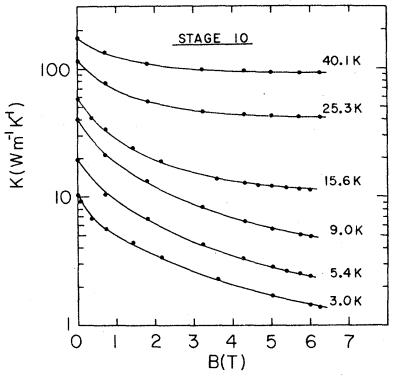

FIG. 6. Magnetothermal conductivity of a stage-10 compound at different temperatures. Log-linear scale is used for display purposes.

ple at different temperatures.

While the electronic thermal conductivity in HOPG is easily suppressed by a few kgauss, we are not able to achieve the same effect on any of the intercalated samples even at 6 tesla. Clearly, the mobilities of the $SbCl_5$ graphites are significantly lower than in HOPG and condition (6) is not fulfilled. A more powerful magnet would be of advantage; nevertheless, it is still doubtful whether even the highest currently available dc fields could fully eliminate the electronic part of the thermal conductivity of low-stage compounds, particularly at elevated temperatures where mobilities are even smaller.

To overcome this difficulty, we make use of an extrapolation technique. The idea is to extrapolate the quantity $\Delta K(B)$, where

$$\Delta K(B) \equiv \Delta K_E(B) = K_E(0) - K_E(B) , \tag{7}$$

from the intermediate to high-field regime using the formula

$$\Delta K(B) = \frac{AB^2}{1+CB^2} , \tag{8}$$

which is asymptotically correct in both low- and high-field regimes, A and C being constants. This method, first proposed by Aliev *et al.*,[21] was successfully applied in the measurements of arsenic[22] and, with certain modifications accounting for large second-order thermomagnetic coefficients, to bismuth.[23] Rewriting (8) in the form

$$\frac{B^2}{\Delta K(B)} = \frac{1}{A} + \frac{CB^2}{A} \tag{9}$$

suggests that the plots of $B^2/\Delta K(B)$ vs B^2 should be linear at all temperatures and the inverse of the slope, $(C/A)^{-1}$, should be equal to the high-field limit,

$$\lim_{B\to\infty} \Delta K(B) ,$$

i.e., to the electronic thermal conductivity $K_E(0)$. An example of such plots for the data of stage-10 compound are illustrated in Fig. 7. Well-defined straight lines justify the use of extrapolation formula (8). From the inverse slopes we get the electronic part of the thermal conductivity shown in Fig. 8 and, using Eq. (5), the lattice thermal conductivity is determined and the results plotted in Fig. 9.

The data of Fig. 8 confirm our expectation of a large enhancement in the electronic part of the thermal conductivity of intercalated compounds. We notice that the increase is about an order of magnitude over a broad temperature range. At the lowest temperatures the temperature dependence of K_E is approximately linear suggesting carrier scattering on impurities and point defects and at about 10 K saturation starts to set in. As a function of stage, the largest electronic thermal conductivity is observed on stage-5 samples, closely followed by a stage-10 compound and, finally, stage-3 samples which have about half as large electronic contribution. Such stage dependence is a result of competition between two important phenomena: Obviously, with larger charge transfer (low stages), more free carriers contribute to the transport and the electronic thermal conductivity should be large. At the same time, however, the graphite matrix is disturbed most when attempting to produce low-

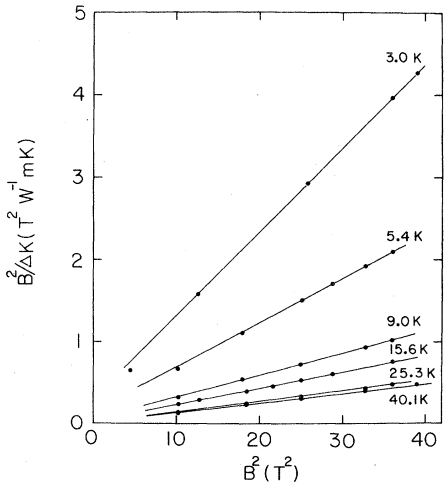

FIG. 7. Plots of $B^2/\Delta K(B)$ vs B^2 for the magnetothermal conductivity data of a stage-10 compound given in Fig. 6. Inverse slope of each line gives the electronic thermal conductivity K_E (see text).

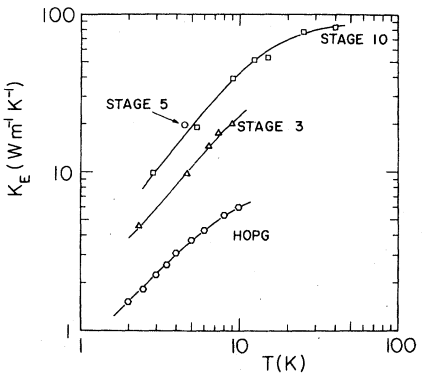

FIG. 8. Temperature dependence of the electronic part of the thermal conductivity, K_E, of $SbCl_5$ graphites and HOPG.

stage compounds and the resulting structural defects provide strong scattering centers for carriers. The balance between these two competing mechanisms gives the optimum contribution which, in our case, occurs near stage 5.

In the liquid-helium temperature range the carrier scattering in HOPG graphite is entirely elastic. This conclusion follows from the inspection of the Wiedemann-Franz ratio,

$$L=\frac{K_E\rho}{T}\ , \tag{10}$$

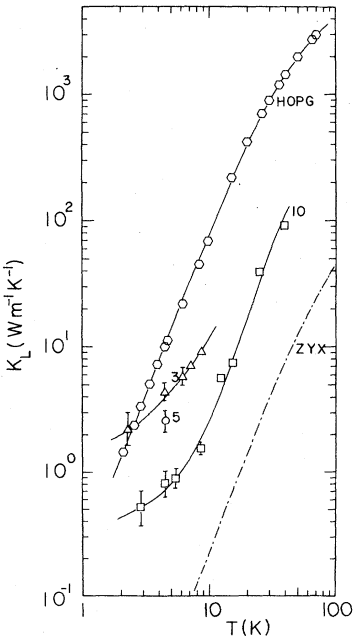

FIG. 9. Temperature dependence of the lattice thermal conductivity of HOPG, $SbCl_5$ graphites, and *ZYX* graphite.

where the Lorentz number L is equal to its Sommerfeld value of $L_0=2.44\times10^{-8}$ V^{2}K^{-2}. This has been first demonstrated by Holland *et al.*[24] and our values of ρ (4.2 K)$=3.18\times10^{-8}$ Ω m and K_E (4.2 K)$=3.2$ W m^{-1}K^{-1} yield $L_0=2.42\times10^{-8}$ V^2K^{-2}, which also confirms this finding. Provided, therefore, that the elastic nature of the carrier scattering in intercalated compounds is preserved, we can estimate, using the Wiedemann-Franz ratio and our data on K_E, the *residual* electrical resistivity of $SbCl_5$ graphites. The values are given in Table I.

An interesting behavior is observed in the lattice thermal conductivity, Fig. 9. Above 4 K, K_L of all intercalated samples is, indeed, substantially smaller than the lattice conductivity of HOPG and this is associated with an additional scattering of phonons on the defect structure of the intercalated compounds. However, one observes a surprising stage dependence of the lattice thermal conductivity as well as a temperature dependence which is very much weaker than the $T^{2.5}$ power law typical of pristine graphite. Intuitively, one would expect the low-temperature lattice thermal conductivity of intercalated graphites to scale with the stage number in a fashion similar to that shown near room temperature; an extra phonon-defect scattering being simply an additional resistive mechanism. The reason why at low temperatures we observe exactly the opposite trend in the stage dependence and a much weaker temperature dependence is, we believe, associated with low-frequency lattice modes in the intercalated compounds. The population of these modes apparently increases with the intercalant concentration and it more than compensates for the phonon-defect scattering. Unfortunately, we are unable to quantify this contribution because, at this time, there is no information available on the dispersion relations of these low-frequency modes. Neutron scattering data would be very useful in this respect.

IV. CONCLUSION

We have made a systematic study of the thermal transport properties of $SbCl_5$ graphite intercalation compounds in the temperature range 2–300 K. The thermopower of all compounds is positive and increases with the stage index. The anomaly on the thermopower curves near 230 K is associated with the commensurate-incommensurate transition. Linear variation of the thermopower at the lowest temperatures is reminiscent of the diffusion trans-

port mechanism. The effect of transverse magnetic field on the thermopower of all compounds is very small primarily due to the reduced mobilities of the intercalated compounds and their high degeneracy.

At high temperatures the thermal conductivity of $SbCl_5$ graphites increases with stage index, nevertheless, the conductivity of all compounds is here substantially smaller than that of the parent material HOPG. However, at liquid-helium range, due to an enhanced electronic part of the thermal conductivity of intercalated compounds, this trend is reversed. Using a strong transverse magnetic field and the extrapolation formula for high-field asymptotic behavior, we have separated the thermal conductivity into its lattice and electronic parts. We observe that the electronic thermal conductivity of GIC's is approximately linear at the lowest temperatures and up to an order of magnitude larger than that of HOPG. Assuming that the carrier scattering remains elastic on intercalation we estimate the residual electrical resistivities of $SbCl_5$ graphites.

At low temperatures the lattice thermal conductivity of all compounds is smaller than that of HOPG but it shows a surprising stage (K_L decreasing with stage index) and temperature dependence. This suggests that we are observing a contribution from the low-frequency lattice modes of the intercalant.

In order to be able to carry out a more detailed analysis of the transport properties of these interesting materials, it is necessary to have information on such fundamental aspects as the shape and multiplicity of their Fermi surfaces and data on the dispersion relation of phonons.

ACKNOWLEDGMENTS

We are grateful to Professor R. Clarke for x-ray characterization of our samples and for useful discussions concerning properties of graphite intercalation compounds. Samples of HOPG were kindly provided by Dr. A. W. Moore of Union Carbide. This research was supported by NSF Grant No. DMR-7924374 and by a grant from the Dow Chemical Company Foundation.

[1]M. S. Dresselhaus and G. Dresselhaus, Adv. Phys. 30, 139 (1981).
[2]J. E. Fischer, in *Physics and Chemistry of Materials with Layered Structure*, edited by F. Lévy (D. Reidel, Dordrecht, 1979), Vol. 6, p. 481.
[3]A. R. Ubbelohde, Carbon 6, 177 (1968).
[4]J. Boxus, B. Poulaert, J.-P. Issi, H, Mazurek, and M. S. Dresselhaus, Solid State Commun. 38, 1117 (1981).
[5]J. Heremans, J.-P. Issi, I. Zabala-Martinez, M. Shayegan, and M. S. Dresselhaus, Phys. Lett. 84A, 387 (1981).
[6]R. Clarke and H. Homma, Bull. Am. Phys. Soc. 26, 452 (1981).
[7]J. Mélin and A. Hérold, Carbon 13, 357 (1975).
[8]P. C. Eklund, J. Giergiel, and P. Boolchand, in *Proceedings of the International Conference on the Physics of Intercalation Compounds, Trieste, 1981,* Vol. 38 of *Springer Series in Solid State Sciences,* edited by L. Pietronero and E. Tosatti (Springer, Berlin, 1981).
[9]R. Clarke, M. Elzinga, J. N. Gray, H. Homma, D. T. Morelli, and C. Uher (unpublished).
[10]R. B. Roberts, Philos. Mag. 36, 91 (1977).
[11]A. D. Caplin, C. K. Chiang, and P. A. Schroeder, Philos. Mag. 30, 1177 (1975).
[12]C. Uher, Phys. Rev. B 25, 4167 (1982).
[13]N. Bartlett, B. McQuillan, and A. S. Robertson, Mater. Res. Bull. 13, 1259 (1978).
[14]F. Batallan, J. Bok, I. Rosenman, and J. Mélin, Phys. Rev. Lett. 41, 330 (1978).
[15]O. Takahashi, Y. Iye, and S. Tanuma, Solid State Commun. 37, 863 (1981).
[16]K. Komatsu, J. Phys. Chem. Solids 25, 707 (1964).
[17]D. G. Onn, L. Q. Wang, Y. Obi, G. Holley, and P. C. Eklund, Bull. Am. Phys. Soc. 27, 405 (1982).
[18]C. A. Klein and M. G. Holland, Phys. Rev. 136, A575 (1964).
[19]T. E. Thompson, E. M. McCarron, and N. Bartlett, Synthetic Metals 3, 255 (1981).
[20]C. Uher, Cryogenics 20, 445 (1980).
[21]S. A. Aliev, L. L. Korenblit, and S. S. Shalyt, Fiz. Tverd. Tela. (Leningrad) 8, 705 (1966), [Sov. Phys.—Solid State 8, 565 (1966)].
[22]C. Uher, J. Phys. F 8, 2559 (1978).
[23]C. Uher and H. J. Goldsmid, Phys. Status Solidi B 65, 765 (1974).
[24]M. G. Holland, C. A. Klein, and W. D. Straub, J. Phys. Chem. Solids 27, 903 (1966).